MATRINE INHIBITS PROLIFERATION AND INVASION OF MOUSE CT26 COLON CANCER CELLS VIA THE P62/PARKIN/PINK1 MITOPHAGY PATHWAY

N. Y. Li[1#*], F. Wang[2#], C. M. Li[3], X. J. Zhang[1], L. Li[4], J. J. Liang[1] and F. Q. Wang[1]

[1]Department of Gastroenterology, The First Hospital of Zhangjiakou, Zhangjiakou, 075000, Hebei, China;
[2]Endoscope Room, The First Hospital of Zhangjiakou, Zhangjiakou, 075000, Hebei, China;
[3]Emergency Management Office, Zhangjiakou Center for Disease Control and Prevention, Zhangjiakou, 075000, Hebei, China;
[4]Department of Nursing, The First Hospital of Zhangjiakou, Zhangjiakou, 075000, Hebei, China.
#These authors contributed equally to this work.
[*]Corresponding author's Email: linanyangny@126.com

ABSTRACT

Matrine, an alkaloid extracted from *Sophora flavescens*, has been shown in recent studies to inhibit colorectal cancer (CRC) progression by regulating mitophagy pathway. This study aimed to investigate whether Matrine affects proliferation of mouse CT26 colon cancer (CC) cells through p62/Parkin/PINK1 signaling axis. CT26 cells were treated with matrine in various concentrations, and proteins related to proliferation, apoptosis, invasion, and epithelial-mesenchymal transition (EMT) was detected. A CT26 tumor-bearing mouse model was fabricated, and mice were rolled into model, positive control, and low-, medium-, and high-dose matrine groups. Tumor weight, inhibition rate, and microvessel density (MVD) were compared, and the expression of EMT and p62/Parkin/PINK1 pathway proteins was examined. Matrine concentration-dependently inhibited cell proliferation, invasion, and cloning, promoted apoptosis, up-regulated E-cadherin, Parkin, and PINK1, and down-regulated N-cadherin, Vimentin, Snail, and p62. In the mouse model, matrine significantly reduced tumor weight and MVD and regulated the expression of the aforementioned proteins. Matrine exerts its anti-CC effects by activating p62/Parkin/PINK1-mediated mitophagy, which induces tumor cell apoptosis and suppresses EMT and angiogenesis. A theoretical basis for understanding mechanism of matrine and its clinical application in treating CC was provided.

Keywords: colon cancer; matrine; proliferation; invasion; EMT; p62/Parkin/PINK1 signaling; mice.

https://doi.org/10.36899/JAPS.2026.4.0083 Published first online May 01, 2026

INTRODUCTION

Colon cancer (CC) is a main cause of cancer-related death (Benson *et al*., 2024). The main treatment methods include surgical resection, supplemented by chemotherapy or radiotherapy. Nevertheless, chemotherapy resistance, postoperative recurrence, and metastasis have seriously affected the clinical treatment effect and prognosis of patients (Tie *et al*., 2022; Gurba *et al*., 2022). Therefore, finding effective strategies to inhibit CC tumor growth has become the focus of research.

Matrine is an alkaloid extracted from *Sophora flavescens*, which has many pharmacological effects, such as anti-inflammatory, anti-fibrosis, antibacterial, and cardioprotective properties (Sun *et al.,* 2022b). In recent years, numerous studies have confirmed its significant antitumor potential. Matrine can improve tumor microenvironment by inhibiting the synthesis and release of inflammatory factors, and then play an anti-cancer role. For example, in breast cancer, matrine can greatly inhibit tumor cell proliferation, block epithelial-mesenchymal transition (EMT), and promote cell apoptosis (Ren *et al.,* 2025). In the mice model of cervical cancer, matrine can inhibited the proliferation of cervical cancer cells and induced autophagy by inhibiting the Akt/mTOR signaling pathway (Zhang *et al.,* 2022). In addition, matrine is reported to down-regulate the expression of p62 and inhibit the proliferation of A549 lung adenocarcinoma cells (Du *et al.,* 2020). Further studies noted that matrine induces mitochondrial dysfunction and activates PTEN-induced kinase 1 (PINK1)/Parkin pathway, thereby regulating mitophagy and contributing to its antitumor effects (Lin *et al.,* 2022; Huang *et al.,* 2025).

In colorectal cancer (CRC), studies also showed the therapeutic potential of matrine. Studies noted that matrine can reduce oxidative stress and inflammatory reaction in colorectal cancer by activating Nrf2 pathway (Dong and Shang,

2025). In addition, matrine down-regulates the expression of AGRIN and inhibits Wnt/β-catenin pathway, thus inhibiting CRC cell activities and inducing apoptosis (Li *et al.,* 2023). The role of PINK1/Parkin pathway in the occurrence of tumors has attracted increasing attention. Autophagy receptor protein p62 recognizes ubiquitinated mitochondrial damage markers through its PB1 domain, and cooperates with Parkin to remove damaged mitochondria. This pathway maintains mitochondrial homeostasis and regulates the survival of colorectal cancer cells (Wang *et al.,* 2024). It is worth noting that imbalance of p62/Parkin/PINK1 pathway is closely related to the malignant progress of CC. This pathway not only affects mitochondrial quality control, but also affects tumor invasion and metastasis by regulating EMT process (Liu *et al.,* 2024). Although matrine may interact with PINK1/Parkin pathway, it is not clear whether it plays an anti-CRC role through p62/Parkin/PINK1 signal axis, and its specific molecular mechanism needs to be clarified.

Given that matrine can regulate the PINK1/Parkin pathway and influence tumor cell proliferation, apoptosis, and EMT, along with its mechanisms of action in other cancer types. This study employed CT26 mouse CC cells to clarify dose-dependent impacts of matrine on proliferation, invasion, apoptosis, and EMT through modulation of the p62/Parkin/PINK1 pathway. A CT26 tumor-bearing mouse model was constructed to investigate effects of matrine on tumor growth and angiogenesis. This study was to provide insights for determining the potential therapeutic targets of CC and further clarify the potential mechanism of matrine's anti-CC effect.

MATERIALS AND METHODS

In vitro cell experiment

Cells culturing and grouping: CT26 mouse CC cell line (Nanjing Kebai Biotechnology Co., Ltd., China) was seeded in RPMI 1640 (+10%FBS and 1%penicillin-streptomycin) (Thermo Fisher, USA), cultured overnight for approximately 16 hours in a Heracell 150i GP humidified incubator (Thermo Fisher, USA) at 37°C with 5% CO_2. Logarithmic growth phase cells were seeded at 5×10^3 cells/well and cultured for 24 hours to allow adherence. Subsequently, medium was replaced with RPMI 1640 medium containing 0.0, 0.5, 1.0, and 2.0 mg/mL matrine (Shanghai Ruichu Biotechnology Co., Ltd., China) for an additional 48 hours of culture. The 0.0 mg/mL group was used as a solvent control group (containing only equal volume of culture medium) to evaluate the basic effect of matrine solvent. All *in vitro* experiments (proliferation, colony formation, invasion, apoptosis, and Western blot) utilized identical medium composition and treatment duration to ensure methodological consistency. Each experiment was repeated three times, and the results were averaged for statistical process.

Cell proliferation and viability assay: At 0, 24, 48, 72, and 96 hours post-treatment, 10 μL CCK-8 reagent (Beyotime Co., Ltd., China) was applied. After further incubation for 1 hour at 37°C, absorbance at 450 nm was measured employing Multiskan FC microplate reader (Thermo Fisher, USA) to assess cell proliferation.

Colony formation assay: After 48 hour-treatment, cells from all groups (including the 0.0 mg/mL matrine control group) were digested with trypsin and counted. Cells were seeded at 500 cells/well and cultured in complete medium (+10% FBS and 1% penicillin-streptomycin) at 37°C and 5% CO_2, with the medium replaced every 3 days for a total of 14 days. When visible cell colonies (defined as clusters of ≥50 cells) formed, the culture was terminated. After medium discarding, cells were gently rinsed twice with pre-cooled PBS, fixed with 4% paraformaldehyde for 10 min at 25°C (Sigma-Aldrich, USA). After the fixative was discarded, cells were stained with 0.5% crystal violet solution (Sigma-Aldrich, USA) for 10 min at 25°C, then excess dye was gently rinsed off, and plates were air-dried. Colony number in each well was observed and counted under an inverted microscope, with three replicate wells per experimental group, and the average values were used for statistical analysis.

Transwell invasion assay: Matrigel matrix (Sigma-Aldrich, USA) was diluted with serum-free medium at a 1:8 volume ratio, mixed thoroughly, and 50 μL was evenly applied to the bottom of the Transwell insert and solidified at 37°C for 2 h. After further culture of CT26 CRC cells from each group for 48 h, a single-cell suspension was prepared at 1×10^5 cells/mL. 250 μL cell suspension was applied to the Matrigel-coated upper chamber, while 600 μL complete medium (10% FBS) was applied to lower chamber. After 48 h-incubation, inserts were removed, and non-invasive cells in upper chamber were gently wiped off. The inserts were fixed with 4% paraformaldehyde for 15 min, stained with 0.5% crystal violet for 10 min, rinsed with PBS, and air-dried at 25°C. Invaded cells were observed under a BioTek Neo2 multi-mode microplate reader (Agilent Technologies, USA), and five random non-overlapping 200× fields were selected to count cell number that had penetrated membrane. The average value was calculated as the number of invasive cells for each sample.

Apoptosis detection: At 48 hour post-treatment, Annexin V-FITC/PI dual staining (reagents sourced from Shanghai Fuyuan Biotechnology Co., Ltd., China) determined cell apoptosis, adhering strictly to supplier's protocol. Briefly,

adherent and floating cells from each treatment group were harvested, subjected to two PBS washes, and reconstituted in ice-cold 1×Binding Buffer at 1×10^6 cells/mL. Aliquots (200 µL) of the suspension were transferred to sterile 5 mL flow tubes, pelleted (1000 ×g, 5 min, 25°C), to remove supernatant. Cell pellet was resuspended in 200 µL of chilled binding buffer, and applied with Annexin V-FITC and PI (5 µL each). Following gentle vortexing, samples were shielded from light for 15 min (25°C). After incubation, 300 µL Binding Buffer was immediately applied, and the samples were analyzed within an hour. CytoFLEX flow cytometer (Beckman Coulter, USA) was utilized to collect 10,000 events per sample, and *FlowJo* (version 10) was employed to analyze the apoptosis rate, including proportions of early and late apoptotic cells.

Each group was compared with a control group (0.0 mg/mL matrine), which was cultured, treated, and analyzed in parallel with the treatment groups to assess the specific effects.

Western blotting: At 48 h post-treatment, cells from each experimental group were harvested. RIPA lysis buffer (Thermo Fisher, USA) extracted proteins, with subsequent quantification via the bicinchoninic acid method (Thermo Fisher, USA). Denaturation was achieved by boiling the protein samples. For immunoblotting, 50 µg of denatured protein per sample was resolved by SDS-PAGE and subsequently electrotransferred onto PVDF membranes (Thermo Fisher, USA) to be blocked for 1 h at 25°C with 5% non-fat dry milk (Shanghai Biotium Biotechnology Co., Ltd., China), followed by TBST washing. Primary antibodies were incubated at 4°C overnight: rabbit monoclonal p62 (1:1000; Abcam, UK), mouse monoclonal Parkin (1:2000; Abcam, UK), rabbit monoclonal PINK1 (1:1000; Biorbyt, UK), and mouse monoclonal GAPDH (1:10000; Abcam, UK). After additional washing with TBST, membrane was treated with HRP-conjugated rabbit anti-mouse IgG secondary antibody (1:10000; Abcam, UK) at 25°C for 1 h. After chemiluminescent detection using enhanced chemiluminescence reagent (Thermo Fisher, USA), the membrane was imaged, and protein band intensities were visualized employing *ImageJ*.

***In vivo* animal experiment**

Animal and grouping: This study utilized fifty 6–8-week-old male BALB/c mice (20–22 g; Beijing Vital River Co., Ltd., China). Animals were maintained under specific-pathogen-free conditions (22±1°C, 55±5% humidity), and received standard rodent diet and water. A standardized 12-h light/dark cycle was implemented throughout the acclimatization and experimental periods. All procedures strictly adhered to the National Institutes of Health guidelines and were approved by Ethics Committee of The First Hospital of Zhangjiakou. Model group (tumor-bearing mice, administered an equal volume of saline by gavage) was taken as the negative control group to visualize the natural tumor progression. The positive control group was treated with cyclophosphamide (CTX) to verify the model's responsiveness to antitumor treatment.

Mice were subjected to tumor modeling following seven days of adaptive feeding. The skin under the right axilla of the mice was disinfected, and CT26 cells in logarithmic growth phase were inoculated at 5×10^6 cells/mL (200 µL). Seven days after successful modeling, mice were randomly rolled into model, positive, Low-dose matrine (LD-M), Middle-dose matrine (MD-M), and High-dose matrine (HD-M) groups. Mice in model group were given gavage with 200 µL of saline. Positive group were given gavage with 25 mg/kg cyclophosphamide. LD-M, MD-M, and HD-M groups were given gavage with 12.5, 25.0, and 50.0 mg/kg matrine, respectively. All groups were given gavage continuously for 14 days.

Observation of mouse general condition: Mouse body weight in each group was measured after 14 days of gavage. Mice were euthanized by cervical dislocation, and tumor tissues were separated, washed clean with saline, dried with filter paper, and weighed. Tumor volume and tumor inhibition rate (TIR) (%) were calculated using equation (1) and (2), respectively:

$$\text{Tumor volume} = \left(\frac{\text{length}+\text{width}}{2}\right)^2 \quad (1)$$

$$\text{TIR}=\frac{\text{Model group}_{\text{average tumor weight}}-\text{Treatment group}_{\text{average tumor weight}}}{\text{Model group}_{\text{average tumor weight}}}\times 100\% \quad (2)$$

Note: TIR reflects percentage decrease in tumor weight in treatment group versus model group, indicating inhibitory effect of the drug on tumor growth.

Immunohistochemical staining: Excised tumor specimens from all experimental groups underwent immediate fixation in 4% paraformaldehyde (Sigma-Aldrich, USA) for 24 h at ambient temperature. Following fixation, a sequential ethanol dehydration series was implemented, made transparent with xylene (Sigma-Aldrich, USA), embedded in paraffin, and sectioned, which were dewaxed in xylene, rehydrated through graded ethanol, and immersed in 3% hydrogen peroxide (Sigma-Aldrich, USA) at 25°C for 10 min, and rinsed with PBS. Sections were incubated with primary antibody against CD34 (Abcam, UK) at 25°C for 30 min, rinsed with PBS. Sections were then stained with diaminobenzidine (Sigma-Aldrich, USA) for 5 min and rinsed with water, then counterstained with hematoxylin (Sigma-Aldrich, USA) for 1 min

and rinsed. After dehydration with graded ethanol and making transparent with xylene, sections were mounted and observed under a microscope. Microvessel density (MVD) was quantified using the Weidner method. First, the sections were systematically scanned at 40× magnification to identify three "hot spot" areas with the highest MVD. Then, for each hot spot, the magnification was switched to 200× (0.785 mm^2/field) to count CD34-positive endothelial cells or cell clusters (excluding vessels with a lumen diameter >50 μm, vessels with a distinct muscular layer, and vessels at the tissue edges or in tissue gaps). Five non-overlapping fields were randomly selected in each hot spot and counted under double-blind conditions (by two independent pathologists; discrepancies >15% were resolved by a third evaluator). The average count of the five fields in each hot spot was calculated, and the overall average of the three hot spot averages was taken as the MVD for that section, as shown in equation (3):

$$MVD = \frac{\sum N_{mic}}{15} \times 0.785(/mm^2) \quad (3)$$

Where $\sum N_{mic}$ represents the number of microvessels in each field.

Western blotting: Tumor tissues from each group were ground in liquid nitrogen, and 1:10 (w/v) pre-chilled radioimmunoprecipitation assay lysis buffer (+1%proteinase inhibitor cocktail) (Thermo Fisher, USA) was added to extract total protein. The samples were then homogenized using an IKA T10 homogenizer (IKA, Germany) at 10,000 rpm in an ice bath for 3 intervals (10 seconds each with a 30-second rest between intervals). Samples were centrifuged at 12,000 g for 15 min at 4°C after incubation on ice, to collect supernatant. BCA quantified protein concentration, adjusted to 2 μg/μL, and then mixed with 5×Loading Buffer (containing β-mercaptoethanol) in a 4:1 ratio. The samples were denatured by heating at 95°C for 5 min in a metal bath (Thermo Fisher, USA). Protein from each sample (40 μg) was loaded into each well, followed by electrophoresis on a 12%SDS-PAGE gel (Bio-Rad, USA) and transfer to PVDF membrane. Primary antibodies for p62, Parkin, PINK1, and GAPDH were consistent with those used in the in vitro experiments. Membrane was incubated with HRP-conjugated secondary antibody (1:10,000; Abcam, UK) for 1 h at 25°C, and underwent ECL detection (Thermo Fisher, USA). Imaging was performed employing Bio-Rad ChemiDoc MP system (USA), and quantitative analysis was conducted employing *ImageJ* (NIH, USA). The experiment was repeated thrice.

Statistical methods: Data were denoted as $\bar{x}\pm s$ and analyzed employing *SPSS 26.0*. All data were tested for normality via Shapiro-Wilk test and for homogeneity of variances via Levene's test. If the assumptions for parametric tests were met, one-way ANOVA with LSD post hoc comparison was applied; otherwise, non-parametric Kruskal-Wallis test was adopted. The significance level was $P<0.05$.

Authors' Contributions: Nanyang Li and Feng Wang designed experiments; Chunmei Li and Xuejun Zhang analyzed data; Lian Li, Jingjing Liang and Fengqiang Wang collected samples; Chunmei Li and Xuejun Zhang performed experiments; Nanyang Li and Feng Wang wrote the manuscript. All authors agreed to publish this article.

RESULTS

Matrine affects proliferation, invasion, and apoptosis of mouse CC cells: Cell proliferation activity is shown in Fig. 1A. With prolonged culture time, the proliferation activity of CT26 CRC cells treated with matrine gradually decreased. Compared with the solvent control group (0.0 mg/mL), the cell proliferation viability in 0.5, 1.0, and 2.0 mg/mL matrine groups showed a concentration-dependent decline. Meanwhile, formed colony number (Fig. 1B), invasive cell number (Figs. 1C, D), and the apoptosis rate (Figs. 1F, G) were all significantly increased. Considerable differences existed among the various matrine treatment groups ($P<0.05$).

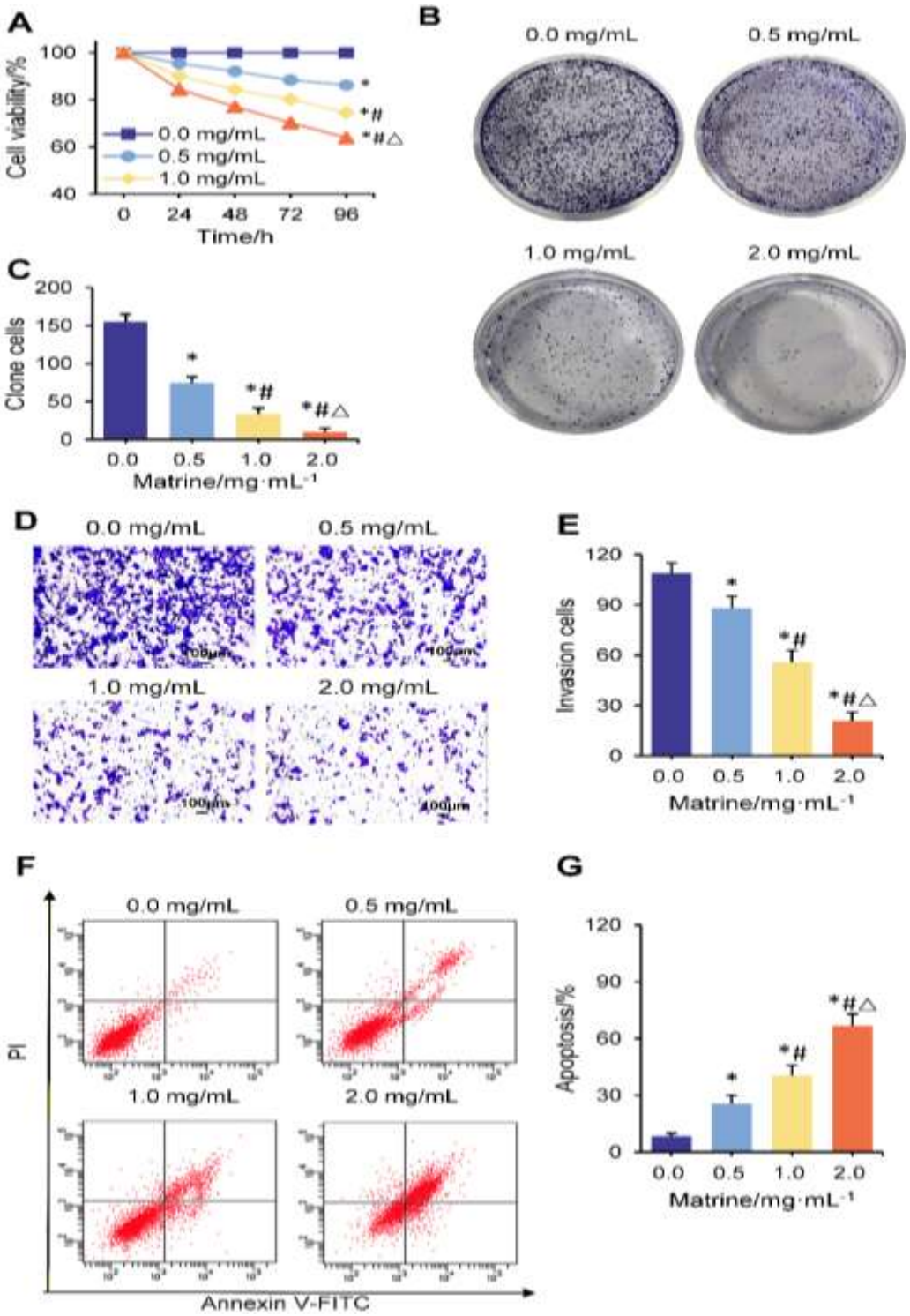

Fig. 1. Matrine affects proliferation, clonal formation, invasion, and apoptosis of colon cancer cells in CT26 mice. A: cell proliferation activity (absorbance at 450 nm) detected by CCK-8 method; B: representative image of cell clone formation experiment (crystal violet staining); C: statistical analysis of the number of clones formed; D: representative image of Transwell invasion experiment (showing transmembrane cells, stained with crystal violet, 100×); E: statistics of transmembrane cell number in transwell chamber; F: flow cytometry-detected apoptosis; G: apoptosis rate statistical analysis. **P*<0.05 *vs.* 0.0mg/mL; #*P*<0.05 *vs.* 0.5mg/mL; Δ*P*<0.05 *vs.* 1.0mg/mL.

Influence of matrine on EMT in mouse CC cells: EMT-related protein levels were detected *in vitro* (Fig. 2A-E). Compared with the solvent control group (0.0 mg/mL), E-cadherin relative protein level in the matrine-treated groups gradually increased with concentration, while N-cadherin, Vimentin, and Snail levels decreased in a dose-dependent manner. Differences among the treatment groups were drastic (P<0.05).

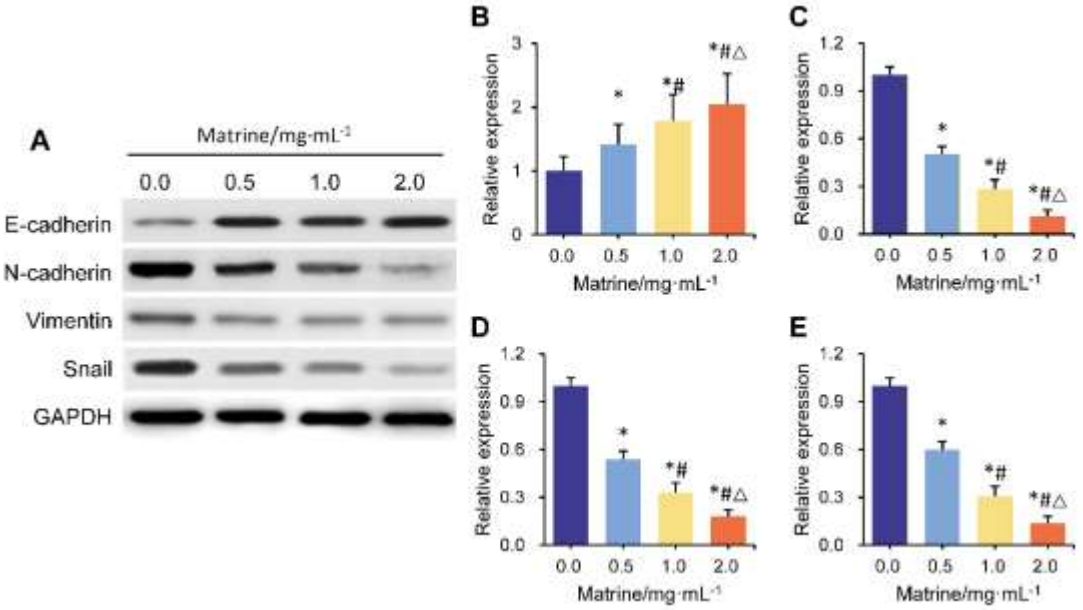

Fig. 2. Matrine impacts expression of EMT-related proteins in mouse CT26 CC cells (Western blot analysis). A: representative Western blot bands of EMT-related proteins; B: E-cadherin; C: N-cadherin; D: Vimentin; E: Snail. **P*<0.05 *vs.* 0.0mg/mL; #*P*<0.05 *vs.* 0.5mg/mL; Δ*P*<0.05 *vs.* 1.0mg/mL.

Impact of matrine on p62/Parkin/PINK1 pathway-related protein relative expression level in CT26 mouse CC cells: The expression levels of proteins associated with the p62/Parkin/PINK1 pathway were assessed *in vitro* (Fig. 3A-D). The outcomes demonstrated that as the concentration of matrine (0.0–2.0 mg/mL) increased, relative protein levels of Parkin and PINK1 in CT26 cells gradually rose, while the expression level of p62 correspondingly decreased. Dramatic differences existed between each concentration treatment group and solvent control group, as well as between adjacent concentration treatment groups (P<0.05).

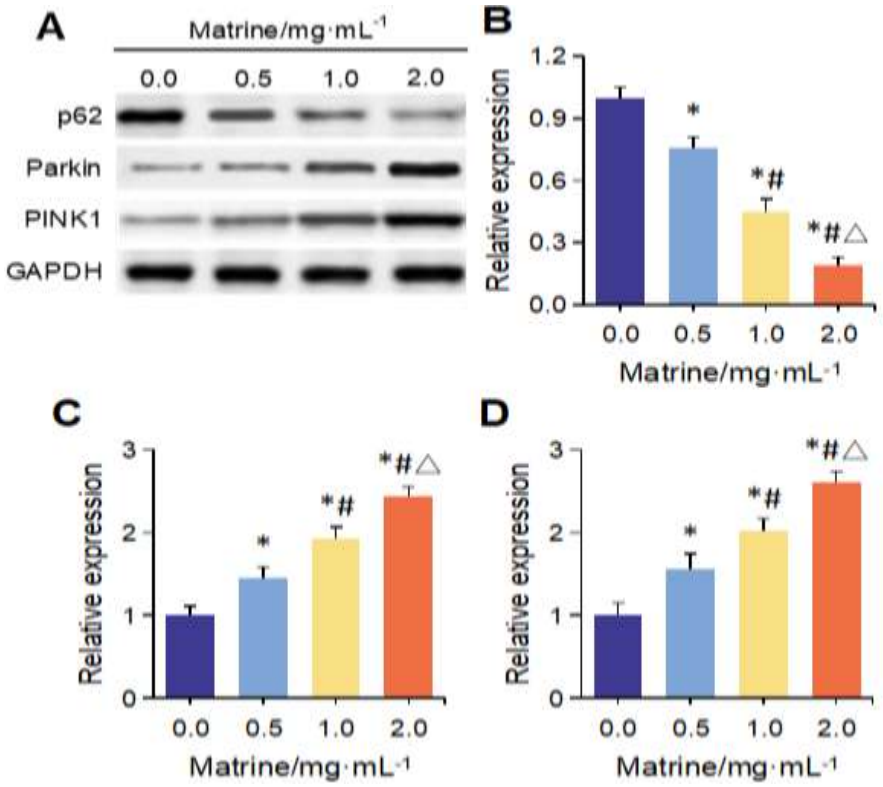

**Fig.3. Impact of matrine on expression of p62/Parkin/PINK1 pathway-related proteins in mouse CT26 CC cells (Western blot analysis). A: representative Western blot bands of p62, Parkin, and PINK1 proteins; B: p62; C: Parkin; D: PINK1. ****P*<0.05 *vs.* 0.0mg/mL; #*P*<0.05 *vs.* 0.5mg/mL; Δ*P*<0.05 *vs.* 1.0mg/mL.

Influence of matrine on tumor growth: In Fig. 4A, slight difference existed in body weight among groups (*P*>0.05). However, tumor weight was reduced in the positive control group and the LD-M, MD-M, and HD-M groups versus model group (*P*<0.05, Fig. 4B). Within the matrine treatment groups, tumor weight decreased with increasing dose, while the tumor inhibition rate correspondingly increased (Fig. 4C). All treatment groups showed dramatic differences (*P*<0.05).

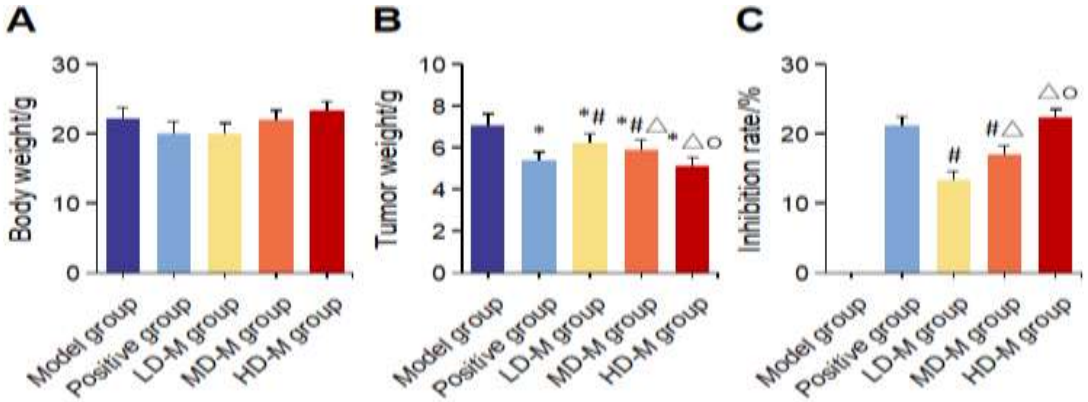

**Fig.4. Evaluation of tumor growth in tumor-bearing mice. A: mice weight; B: tumor weight; C: TIR calculated based on tumor weight. ****P*<0.05 *vs.* model group; #*P*<0.05 *vs.* positive group; Δ*P*<0.05 *vs.* LD-M group; ○ *P*<0.05 *vs.* MD-M group.

Effect of matrine on MVD in tumor tissues: Immunohistochemical staining of tumor tissues and evaluation of MVD showed (Fig. 5A-B) that the tumor MVD in the positive control group and all matrine dose groups was inferior to model

group (P<0.05). Furthermore, MVD in the matrine treatment groups exhibited a dose-dependent decreasing trend, and the differences among the dose groups were great (P<0.05).

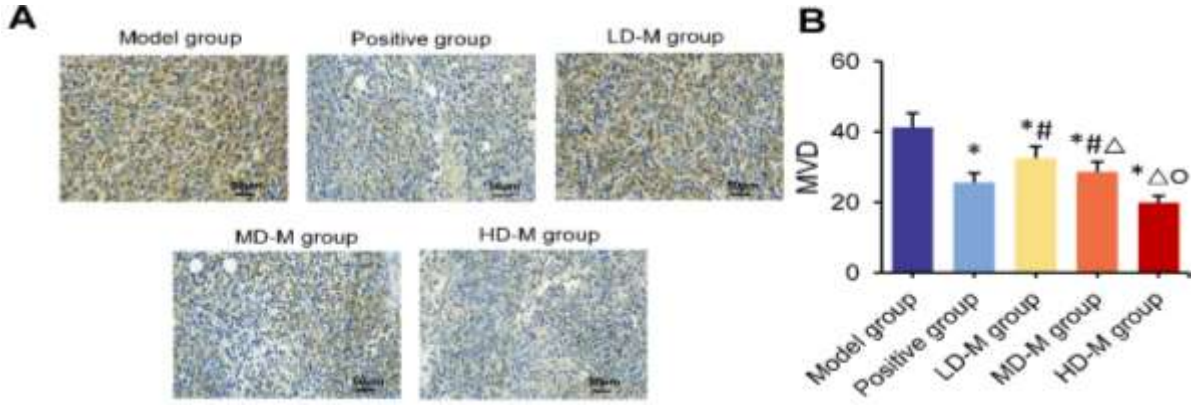

Fig.5. Influence of matrine on tumor tissue MVD in CT26 tumor bearing mice. A: representative image of tumor tissue CD34 immunohistochemical staining (used for MVD counting, 400×); B: MVD statistical results. *P<0.05 *vs.* model group; #P<0.05 *vs.* positive group; ΔP<0.05 *vs.* LD-M group; ○P<0.05 *vs.* MD-M group.

Effect of matrine on EMT: The expression of EMT-related proteins in tumor tissues is presented in Fig. 6A-E. E-cadherin relative protein level was higher in positive control group and all matrine dose groups versus model group, while N-cadherin, Vimentin, and Snail were lower (P<0.05). Within matrine treatment groups, E-cadherin levels increased with the dose, while the levels of the other three proteins decreased accordingly, with drastic differences observed among the groups (P<0.05).

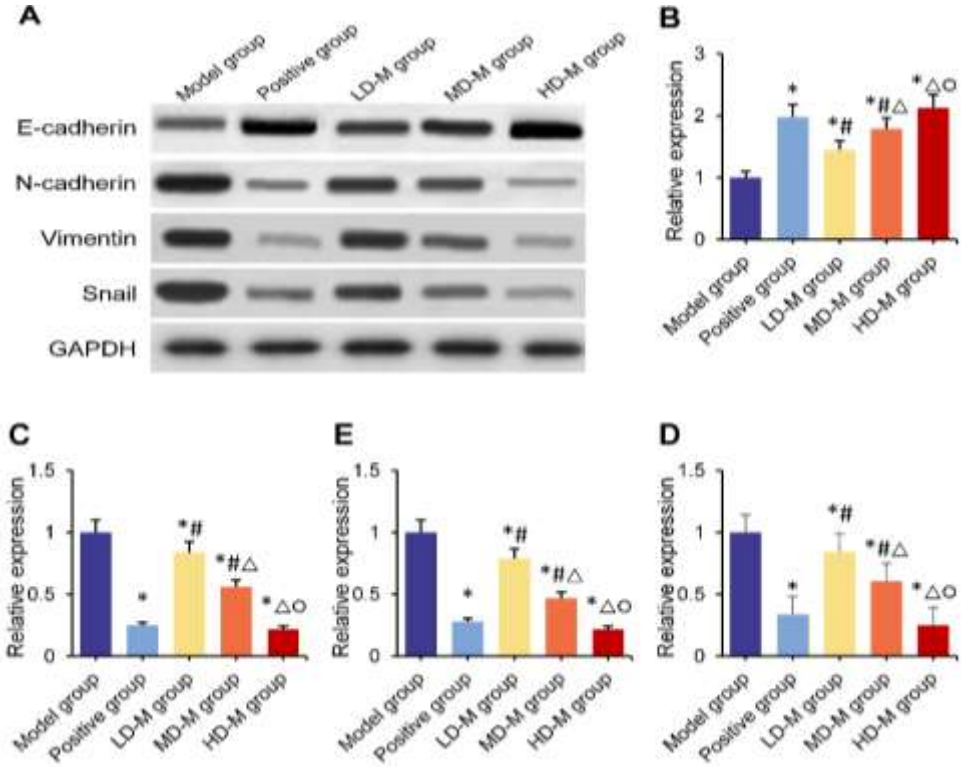

Fig.6. Impact of matrine on EMT-related protein levels in tumor tissues of CT26 tumor bearing mice (Western blot analysis). A: representative Western blot bands of EMT related proteins; B: E-cadherin; C: N-cadherin; D: Vimentin; E: Snail. *P<0.05 *vs.* model group; #P<0.05 *vs.* positive group; ΔP<0.05 *vs.* LD-M group; ○P<0.05 *vs.* MD-M group.

Matrine affects p62/Parkin/PINK1 pathway-related protein levels in tumors: The evaluation of protein expression related to the p62/Parkin/PINK1 pathway in tumor tissues is shown in Fig. 7A-D. p62 protein level was lower in positive control group and all matrine dose groups versus model group, while Parkin and PINK1 protein levels were higher (P<0.05). Within matrine treatment groups, p62 expression showed a dose-dependent downregulation, whereas Parkin and PINK1 expression exhibited a dose-dependent upregulation. All differences among the treatment groups were considerable (P<0.05).

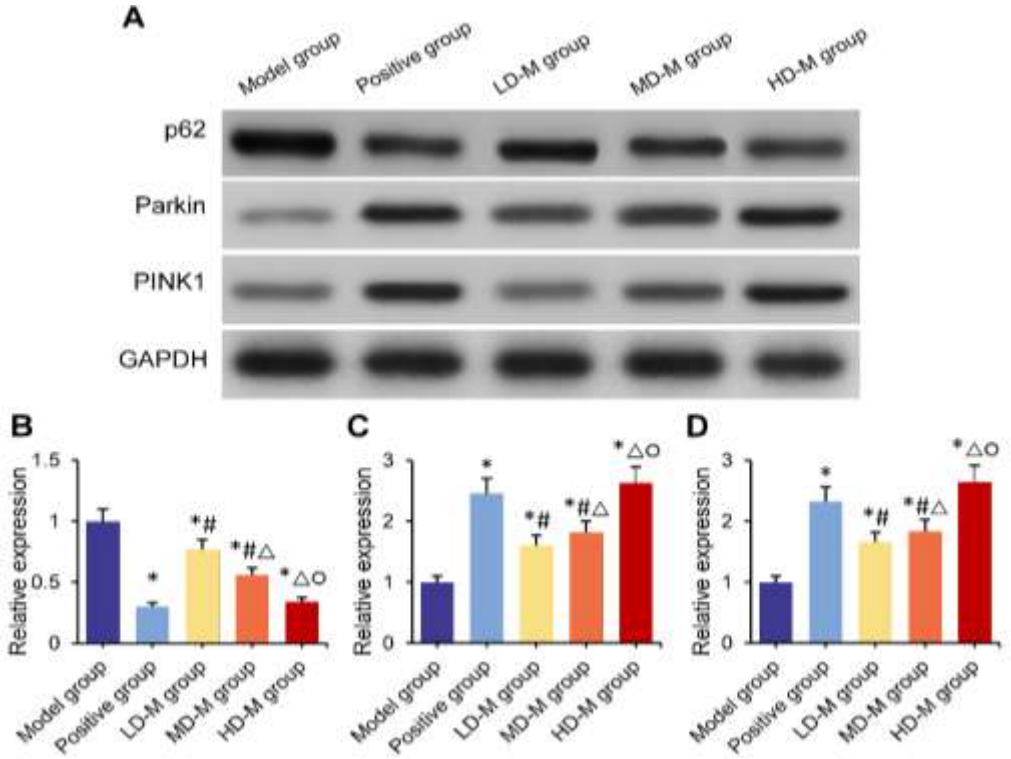

Fig.7. Matrine affects expression of p62/Parkin/PINK1 pathway-related proteins in tumor tissues of CT26 tumor bearing mice (Western blot analysis). A: representative Western blot bands of p62, Parkin, and PINK1 proteins; B: p62; C: Parkin; D: PINK1. *P<0.05 *vs.* model group; #P<0.05 *vs.* positive group; ΔP<0.05 *vs.* LD-M group; ○P<0.05 *vs.* MD-M group.

DISCUSSION

This study indicated that matrine inhibits proliferation, colony formation, and invasion ability of CT26 mouse CRC cells in a concentration dependent manner. Matrine administration greatly reduced the tumor weight of tumor-bearing mice and improved the tumor inhibition rate, showing a dose-dependent effect.

Matrine is an alkaloid extracted from Sophora flavescens, which has antiviral, immunomodulatory, and anticancer activities (Chhabra and Mehan, 2023; Li *et al*., 2021; Sun *et al*., 2022). It is worth noting that besides directly inhibiting the activity of tumor cells, the anticancer effect of matrine may involve multi-channel regulation. For example, Du *et al.* (2023) found that matrine can inhibit the formation of vascular-like structures and induce apoptosis in CT26 cells. The results confirmed that matrine can dose dependently reduce microvascular density in tumor tissues, indicating that anti angiogenesis is one of the mechanisms of its anti-tumor activity *in vivo*.

To further clarify the anticancer mechanism of matrine, effect of matrine on EMT was also analyzed in this work. EMT is the key process of tumor metastasis, which can enhance the invasion and dryness of cells (Taki *et al.*, 2021; Manfioletti and Fedele, 2023). Matrine down-regulated N-cadherin, vimentin and Snail levels in CT26 cells and tumor tissues in a dose-dependent manner, while up-regulated the expression of E- cadherin. Sang *et al.* reported the similar finding in a breast cancer model, which suggested that the inhibition of EMT may be a common mechanism underlying the broad-spectrum anticancer effects of matrine (Sang *et al.*, 2025). E- cadherin is an adhesion molecule between epithelial markers and epithelial cells, which maintains the integrity and polarity of epithelium (Yang *et al.*, 2023). E- cadherin, as an epithelial marker, is very necessary to maintain the adhesion of epithelial cells. Its low

expression is a landmark event of EMT and can promote the migration of CC cells (Vazquez-Carretero *et al.*, 2021). In contrast, upregulation of N-cadherin and Vimentin, along with the activation of the transcription factor Snail, further enhances tumor invasiveness (Skarkova *et al.*, 2022; Aborisade *et al.*, 2022).

In addition to regulating EMT and angiogenesis, this study is the first to find that matrine can also inhibit CRC progression by influencing mitophagy through the p62/Parkin/PINK1 pathway. The p62/Parkin/PINK1 pathway acts as a "molecular switch" in regulating cellular response to many stressors, and it primarily participates in the process of mitophagy (Olszewska *et al*., 2022). Mitochondrial autophagy can selectively remove damaged mitochondria, thus maintaining cell homeostasis, preventing oxidative stress, and reducing the accumulation of harmful substances (Zhang *et al*., 2022). The expression of PINK1 is generally lower in CRC tissue than in normal tissues (Arcos *et al*., 2025). PINK1 recruits and activates Parkin, which ubiquitinates mitochondrial proteins such as VDAC1 and Mfn1/2, thus inducing mitochondrial autophagy (Quinn *et al.*, 2020). p62 binds to the ubiquitinated substrate and bridges it to LC3-positive autophagy for degradation (Thinwa *et al*., 2024). The imbalance of p62/Parkin/PINK1 pathway will damage mitochondrial phagocytosis, resulting in the failure to clear the damaged mitochondria in time. This will lead to the excessive production of ROSs and other harmful substances, which will affect the cancer occurrence and metastasis (Mao *et al*., 2021; Miyazaki *et al*., 2022).

Matrine markedly inhibits p62 protein expression but promotes the protein expression of Parkin and PINK1. However, the regulation of matrine on autophagy is complex and environmentally dependent. In some tumors, it activates autophagy; In other tumors, such as pancreatic cancer with KRAS mutation, it inhibits autophagy by damaging lysosomal function, thus inhibiting tumor growth (Cho *et al.*, 2018). Lei *et al.* (2020) found that increased p62 levels in CRC tissues are an independent prognostic factor for poor outcomes, which clinically supports the potential therapeutic value of matrine-induced p62 downregulation observed in this study.

In summary, matrine inhibits CRC by directly inhibiting proliferation and anti-angiogenesis, reversing EMT, and activating mitochondrial autophagy through p62/Parkin/PINK1 axis to induce apoptosis. These interrelated mechanisms work together to form the basis of matrine's anti-CRC effect, and provide a solid theoretical basis for its development as a multi-target natural anti-tumor drug.

Conclusion: Matrine inhibited CT26 mouse CC cell proliferation and invasion while promote apoptosis, with concentration-dependent characteristics. Matrine also inhibited tumor growth and angiogenesis in CC. Such effect was mainly achieved by influencing E-cadherin, N-cadherin, Vimentin, and Snail protein to suppress the EMT in mouse CC cells. Additionally, matrine mediated the p62/Parkin/PINK1 signaling pathway to affect mitochondrial autophagy, thereby exerting its anti-CC effects. In conclusion, this work provides potential mechanisms underlying matrine's anti-CC activity and offer valuable information for finding novel therapeutic approaches for CC.

REFERENCES

Arcos, M., L. Goodla, H. Kim, S.P. Desai, R. Liu, K. Yin, Z. Liu, D.R. Martin and X. Xue (2025). PINK1-deficiency facilitates mitochondrial iron accumulation and colon tumorigenesis. Autophagy. 21(4): 737-753. https://doi.org/10.1080/15548627.2024.2425594

Beck, M., M. Baranger, A. Moufok-Sadoun, E. Bersuder, I. Hinkel, G. Mellitzer, E. Martin, L. Marisa, I. Duluc, A. de Reynies, C. Gaiddon, J.N. Freund and I. Gross (2021). The atypical cadherin MUCDHL antagonizes colon cancer formation and inhibits oncogenic signaling through multiple mechanisms. Oncogene. 40(3): 522–535. https://doi.org/10.1038/s41388-020-01546-y

Benson, A.B., A.P. Venook, M. Adam, G. Chang, Y.J. Chen, K.K. Ciombor, S.A. Cohen, H.S. Cooper, D. Deming, I. Garrido-Laguna, J.L. Grem, P. Haste, J.R. Hecht, S. Hoffe, S. Hunt, H. Hussan, K.L. Johung, N. Joseph, N. Kirilcuk, S. Krishnamurthi, M. Malla, J.K. Maratt, W.A. Messersmith, J. Meyerhardt, E.D. Miller, M.F. Mulcahy, S. Nurkin, M.J. Overman, A. Parikh, H. Patel, K. Pedersen, L. Saltz, C. Schneider, D. Shibata, B. Shogan, J.M. Skibber, C.T. Sofocleous, A. Tavakkoli, C.G. Willett, C. Wu, L.A. Gurski, J. Snedeker and F. Jones (2024). Colon Cancer, Version 3.2024, NCCN Clinical Practice Guidelines in Oncology. J Natl Compr Canc Netw. 22(2 D): e240029. https://doi.org/10.6004/jnccn.2024.0029

Chhabra, S. and S. Mehan (2023). Matrine exerts its neuroprotective effects by modulating multiple neuronal pathways. Metab Brain Dis. 38(5): 1471–1499. https://doi.org/10.1007/s11011-023-01214-6

Cho, Y. R., J. H. Lee, J. H. Kim, S. Y. Lee, S. Yoo, M. K. Jung, S. J. Kim, H. J. Yoo, C. G. Pack, J. K. Rho and J. Son (2018). Matrine suppresses KRAS-driven pancreatic cancer growth by inhibiting autophagy-mediated energy metabolism. Mol Oncol. 12(7): 1203–1215. https://doi.org/10.1002/1878-0261.12324

Dong, Y. F. and T. Shang (2025). Matrine Alleviates Oxidative Stress and Inflammation in Colon Cancer by Activating the Nrf2 Pathway. Turk J Gastroenterol. 36(9): 563-572. https://doi.org/10.5152/tjg.2025.24438

Du, J., J. Li, D. Song, Q. Li, L. Li, B. Li, and L. Li (2020). Matrine exerts anti-breast cancer activity by mediating apoptosis and protective autophagy via the AKT/mTOR pathway in MCF-7 cells. Mol Med Rep. 22(5): 3659–3666. https://doi.org/10.3892/mmr.2020.11449

Du, Q., Y. Lin, C. Ding, L. Wu, Y. Xu and Q. Feng (2023). Pharmacological Activity of Matrine in Inhibiting Colon Cancer Cells VM Formation, Proliferation, and Invasion by Downregulating Claudin-9 Mediated EMT Process and MAPK Signaling Pathway. Drug Des Devel Ther. 17: 2787–2804. https://doi.org/10.2147/DDDT.S417077

Gurba, A., P. Taciak, M. Sacharczuk, I. Młynarczuk-Biały, M. Bujalska-Zadrożny and J. Fichna (2022). Gold (III) Derivatives in Colon Cancer Treatment. Int J Mol Sci. 23(2): 724. https://doi.org/10.3390/ijms23020724

Huang, B., Y. Yang, J. Liu, B. Zhang and N. Lin (2025). Ubiquitination regulation of mitochondrial homeostasis: a new sight for the treatment of gastrointestinal tumors. Front Immunol. 16: 1533007. https://doi.org/10.3389/fimmu.2025.1533007

Jin, J., Z. Fan, Y. Long, Y. Li, Q. He, Y. Yang, W. Zhong, D. Lin, D. Lian, X. Wang, J. Xiao and Y. Chen (2024). Matrine induces ferroptosis in cervical cancer through activation of piezo1 channel. Phytomedicine. 122: 155165. https://doi.org/10.1016/j.phymed.2023.155165

Lei, C., B. Zhao, L. Liu, X. Zeng, Z. Yu and X. Wang (2020). Expression and clinical significance of p62 protein in colon cancer. Medicine (Baltimore). 99(3): e18791. https://doi.org/10.1097/MD.0000000000018791

Li, X., Y. Lu, P. Wen, Y. Yuan, Z. Xiao, H. Shi and E. Feng (2023). Matrine restrains the development of colorectal cancer through regulating the AGRN/Wnt/β-catenin pathway. Environ Toxicol. 38(4): 809–819. https://doi.org/10.1002/tox.23730

Li, X., Z. Tang, L. Wen, C. Jiang and Q Feng (2021). Matrine: A review of its pharmacology, pharmacokinetics, toxicity, clinical application and preparation researches. J Ethnopharmacol. 269: 113682. https://doi.org/10.1016/j.jep.2020.113682

Lin, Y., F. He, L. Wu, Y. Xu and Q. Du (2022). Matrine Exerts Pharmacological Effects Through Multiple Signaling Pathways: A Comprehensive Review. Drug Des Devel Ther. 16: 533–569. https://doi.org/10.2147/DDDT.S349678

Liu, H., Y. Huang, C. Zhao, G. Wang and X. Wang (2024). ABALON regulates mitophagy and 5-FU sensitivity in colorectal cancer via PINK1-Parkin pathway. Transl Cancer Res. 13(11): 6201–6218. https://doi.org/10.21037/tcr-24-933

Manfioletti, G. and M. Fedele (2023). Epithelial-Mesenchymal Transition (EMT). Int J Mol Sci. 24(14): 11386. https://doi.org/10.3390/ijms241411386

Mao, L., H. Liu, R. Zhang, Y. Deng, Y. Hao, W. Liao, M. Yuan and S. Sun (2021). PINK1/Parkin-mediated mitophagy inhibits warangalone-induced mitochondrial apoptosis in breast cancer cells. Aging (Albany NY). 13(9): 12955–12972. https://doi.org/10.18632/aging.202965

Miyazaki, N., R. Shiratori, T. Oshima, Z. Zhang, R. Valencia, J. Kranrod, L. Fang, J.M. Seubert, K. Ito and S. Aoki (2022). PINK1-dependent and Parkin-independent mitophagy is involved in reprogramming of glycometabolism in pancreatic cancer cells. Biochem Biophys Res Commun. 625: 167–173. https://doi.org/10.1016/j.bbrc.2022.08.004

Olszewska, D.A., A. McCarthy, A.I. Soto-Beasley, R.L. Walton, O.A. Ross and T. Lynch (2022). PARKIN, PINK1, and DJ1 analysis in early-onset Parkinson's disease in Ireland. Ir J Med Sci. 191(2): 901–907. https://doi.org/10.1007/s11845-021-02563-w

Quinn, P.M.J., P.I. Moreira, A.F. Ambrósio and C.H. Alves (2020). PINK1/PARKIN signalling in neurodegeneration and neuroinflammation. Acta Neuropathol Commun. 8(1): 189. https://doi.org/10.1186/s40478-020-01062-w

Ren, L., Z. Fang, J. Xu, X. Wu, Y. Zhang, H. Cai and Z. Han (2025). Matrine Inhibits Breast Cancer Cell Proliferation and Epithelial-Mesenchymal Transition Through Regulating the LINC01116/miR-9-5p/ITGB1 Axis. Balkan Med J. 42(1): 54–65. https://doi.org/10.4274/balkanmedj.galenos.2024.2024-8-49

Sang, Y., Y. Hu, R. Liang, Y. Zhang, H. Du, H. Zhang, J. Chen, Y. Zhang and X. Cao (2025). Matrine targets β-catenin and blocks the formation of β-catenin/TCF7L2 complex to promote ferroptosis and inhibit metastasis in triple-negative breast cancer. Phytomedicine. 145: 157044. https://doi.org/10.1016/j.phymed.2025.157044

Skarkova, V., B. Vitovcova, P. Matouskova, M. Manethova, P. Kazimirova, A. Skarka, V. Brynychova, P. Soucek, H. Vosmikova and E. Rudolf (2022). Role of N-Cadherin in Epithelial-to-Mesenchymal Transition and Chemosensitivity of Colon Carcinoma Cells. Cancers (Basel). 14(20): 5146. https://doi.org/10.3390/cancers14205146

Sun, X.Y., L.Y. Jia, Z. Rong, X. Zhou, L.Q. Cao, A.H. Li, M. Guo, J. Jin, Y.D. Wang, L. Huang, Y.H. Li, Z.J. He, L. Li, R.K. Ma, Y.F. Lv, K.K. Shao, J. Zhang and H.L. Cao (2022a). Research Advances on Matrine. Front Chem. 10: 867318. https://doi.org/10.3389/fchem.2022.867318

Sun, Y., L. Xu, Q. Cai, M. Wang, X. Wang, S. Wang and Z. Ni (2022b). Research progress on the pharmacological effects of matrine. Front Neurosci. 16: 977374. https://doi.org/10.3389/fnins.2022.977374

Taki, M., K. Abiko, M. Ukita, R. Murakami, K. Yamanoi, K. Yamaguchi, J. Hamanishi, T. Baba, N. Matsumura and M. Mandai (2021). Tumor Immune Microenvironment during Epithelial-Mesenchymal Transition. Clin Cancer Res. 27(17): 4669–4679. https://doi.org/10.1158/1078-0432.CCR-20-4459

Thinwa, J.W., Z. Zou, E. Parks, S. Sebti, K. Hui, Y. Wei, M. Goodarzi, V. Singh, G. Urquhart, J.L. Jewell, J.K. Pfeiffer, B. Levine, T.A. Reese and M.U. Shiloh (2024). CDKL5 regulates p62-mediated selective autophagy and confers protection against neurotropic viruses. J Clin Invest. 134(1): e168544. https://doi.org/10.1172/JCI168544

Tie, J., J.D. Cohen, K. Lahouel, S.N. Lo, Y. Wang, S. Kosmider, R. Wong, J. Shapiro, M. Lee, S. Harris, A. Khattak, M. Burge, M. Harris, J. Lynam, L. Nott, F. Day, T. Hayes, S.A. McLachlan, B. Lee, J. Ptak, N. Silliman, L. Dobbyn, M. Popoli, R. Hruban, A.M. Lennon, N. Papadopoulos, K.W. Kinzler, B. Vogelstein, C. Tomasetti, P. Gibbs and DYNAMIC Investigators (2022). Circulating Tumor DNA Analysis Guiding Adjuvant Therapy in Stage II Colon Cancer. N Engl J Med. 386(24): 2261–2272. https://doi.org/10.1056/NEJMoa2200075

Vazquez-Carretero, M.D., P. García-Miranda, M.S. Balda, K. Matter, A.A. Ilundáin and M.J. Peral (2021). Proper E-cadherin membrane location in colon requires Dab2 and it modifies by inflammation and cancer. J Cell Physiol. 236(2): 1083–1093. https://doi.org/10.1002/jcp.29917

Wang, Y., Y. Liu, X. Su, L. Niu, N. Li, C. Xu, Z. Sun, H. Guo, S. Shen and M. Yu (2024). Non-pathogenic Trojan horse Nissle1917 triggers mitophagy through PINK1/Parkin pathway to discourage colon cancer. Mater Today Bio. 29: 101273. https://doi.org/10.1016/j.mtbio.2024.101273

Yang, H., G.G. Yue, K.K. Yuen, S. Gao, P.C. Leung, C.K. Wong and C.B. Lau (2023). Mechanistic insights into the anti-tumor and anti-metastatic effects of Patrinia villosa aqueous extract in colon cancer via modulation of TGF-β R1-smad2/3-E-cadherin and FAK-RhoA-cofilin pathways. Phytomedicine. 117: 154900. https://doi.org/10.1016/j.phymed.2023.154900

Zhang, F., H. Zhang, W. Qian, Y. Xi, L. Chang, X. Wu and M. Li (2022). Matrine exerts antitumor activity in cervical cancer by protective autophagy via the Akt/mTOR pathway *in vitro* and *in vivo*. Oncol Lett. 23(4): 110. https://doi.org/10.3892/ol.2022.13230.

Zhang, K., D. Zhang, J. Wang, Y. Wang, J. Hu, Y. Zhou, X. Zhou, S. Nie and M. Xie (2022). Aloe gel glucomannan induced colon cancer cell death via mitochondrial damage-driven PINK1/Parkin mitophagy pathway. Carbohydr Polym. 295: 119841. https://doi.org/10.1016/j.carbpol.2022.119841